THE JOURNAL OF PHYSICAL CHEMISTRY LETTERS
A JOURNAL OF THE AMERICAN CHEMICAL SOCIETY

pubs.acs.org/JPCL Letter

# Existence of Acetaldehyde Clathrate Hydrate and Its Dissociation Leading to Cubic Ice under Ultrahigh Vacuum and Cryogenic Conditions

Gaurav Vishwakarma, Bijesh K. Malla, Soham Chowdhury, Sakshi Pradip Khandare, and Thalappil Pradeep*

Cite This: J. Phys. Chem. Lett. 2023, 14, 5328−5334 Read Online

ACCESS | Metrics & More | Article Recommendations | Supporting Information

**ABSTRACT:** Acetaldehyde in a dilute aqueous solution gets hydrated to produce a geminal diol under atmospheric conditions. The acetaldehyde−water ice system under high pressure also converts to a geminal diol, and therefore, its stable clathrate hydrate (CH) phase, which in most systems forms at high pressures, is unknown. In the present study, we showed that acetaldehyde CH exists in ultrahigh vacuum ($10^{-10}$ mbar) under cryogenic conditions (below 140 K) and continues to exist at 115 K for periods well over 1 day. Decomposition of acetaldehyde CH at 130−135 K produces water ice in its cubic crystalline form. The mechanism and kinetics involved in the process have also been studied. Reflection absorption infrared spectroscopy and temperature-programmed desorption mass spectrometry were utilized to confirm the CH formation. Our study establishes the possibility of a stable CH phase for acetaldehyde in interstellar and cometary environments.

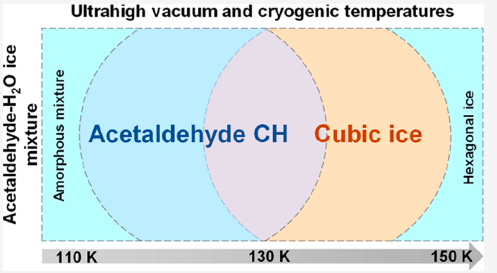


The existence of the clathrate hydrates (CHs) of several simple molecules in ultrahigh vacuum (UHV) and cryogenic conditions is now well established; examples include $CH_4$,[1] $CO_2$,[1,2] $C_2H_6$,[3] acetone,[4] formaldehyde,[5] and THF.[2,6] Some of these CHs dissociate leading to cubic ice (ice $I_c$),[4] while others form hexagonal ice (ice $I_h$),[5] although CH to crystalline ice transformation under high-pressure conditions was known even earlier.[7−12] Exploration of CH phases in vacuum conditions continues with various simple molecules.[13] An important possibility is the occurrence of unique CH phases for certain molecules, hitherto unknown.

CHs are a class of host−guest compounds wherein water within its hydrogen-bonded cages hosts guest molecules such as $CH_4$, $CO_2$, $H_2S$, etc.[14] Depending on the molecular size and chemical behavior of guest molecules, these CHs are known to exist mainly in two structures, namely structure I (sI) and structure II (sII). Such structures exist at moderately low temperatures and high pressures. However, until now, a stable CH phase of acetaldehyde has not been observed.[15,16] This is because acetaldehyde in dilute aqueous solution and in the solid state converts to a geminal diol under atmospheric pressure.[15,17] The hydration of acetaldehyde to a geminal diol was confirmed by calorimetric and spectrophotometric methods.[17−19] Even incorporating a "help guest" to stabilize the acetaldehyde CH was found to be ineffective, as it became a geminal diol under high pressure. However, the geminal diol formed was subsequently transformed to its CH phase under a high pressure of 120 bar at 253.[16] In view of this thermodynamically stable geminal diol, the existence of acetaldehyde CH has not been observed so far. We thought it instructive to explore the existence of acetaldehyde CH in UHV and cryogenic conditions.

Water ice is pervasive in terrestrial and extraterrestrial environments and exists in various amorphous and crystalline forms.[20,21] Among the all-crystalline forms, ice $I_h$ is the most stable and prevalent crystalline form of ice under Earth's conditions.[22] However, the preparation and study of ice $I_c$ have drawn close attention of the scientific community due to its importance to extraterrestrial environments, Earth's atmosphere, cryopreservation, and climate change.[9,23−26] Among the main established routes for forming ice $I_c$,[26] studying its formation via CH dissociation under UHV and cryogenic conditions will be of importance for cometary and interstellar environments.[4,27,28]

In the following, we present a systematic study of the transformation of acetaldehyde in its water ice mixture to its CH phase at 115 K. This transformation was studied by reflection absorption infrared spectroscopy (RAIRS) and temperature-programmed desorption mass spectrometry (TPD-MS). Further, the dissociation of acetaldehyde CH at

Received: May 1, 2023
Accepted: June 1, 2023







https://doi.org/10.1021/acs.jpclett.3c01181
J. Phys. Chem. Lett. 2023, 14, 5328−5334

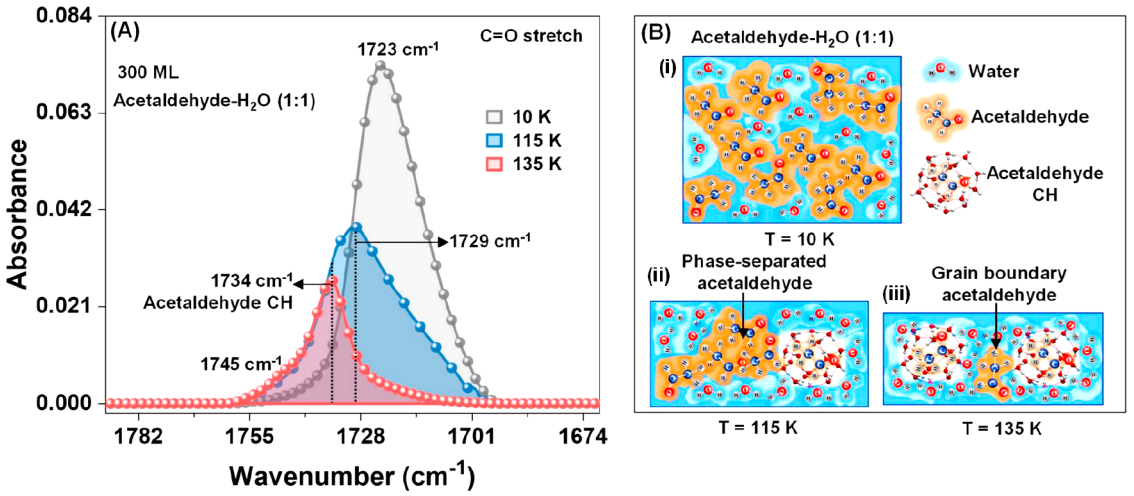


**Figure 1.** Formation of acetaldehyde CH under UHV conditions, as observed using the C=O stretching region. (A) Temperature-dependent RAIR spectra of 300 ML of acetaldehyde−$H_2O$ (1:2) film in the C=O stretching region. The peaks at 1729 and 1734 $cm^{-1}$ are marked by vertical dashed lines. The ice mixture was codeposited on a Ru(0001) substrate at 10 K and annealed at a rate of 2 K·$min^{-1}$ to the set temperatures. (B) Schematic representation of stepwise evolution of ice mixture upon thermal annealing. Change in the thickness of the composite film is a result of acetaldehyde desorption, as implied in (i−iii).

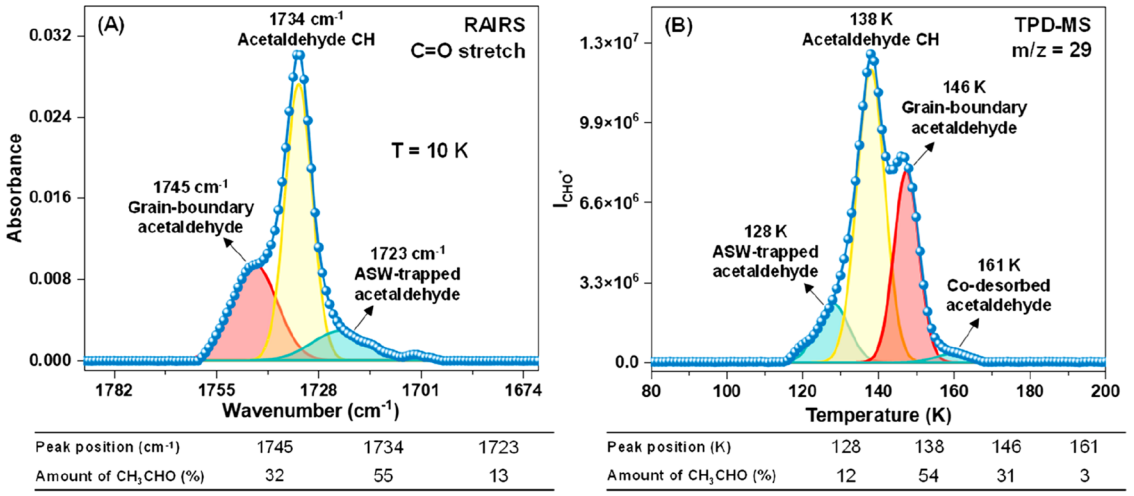


**Figure 2.** (A) RAIR spectrum of 300 ML of acetaldehyde−$H_2O$ (1:2) film at 10 K in the C=O stretching region, after forming CH. For this measurement, the ice mixture was prepared by codeposition on a Ru(0001) substrate at 10 K and annealed at a rate of 2 K·$min^{-1}$ to 137 K to form acetaldehyde CH. The resulting ice at 137 K was cooled to 10 K, and the RAIR spectrum was measured. The C=O stretching band was deconvoluted to estimate the fractions of different phases of acetaldehyde in the $H_2O$ matrix. (B) TPD-MS spectrum of the same system. After RAIRS data acquisition at 10 K, the TPD-MS spectrum was collected by annealing the substrate at a rate of 30 K·$min^{-1}$ to 200 K. In the spectrum, the intensity of $CHO^+$ ($m/z$ = 29) is plotted as a function of substrate temperature. The TPD spectrum in the temperature window of 80−200 K was deconvoluted to estimate the different fractions of acetaldehyde in the $H_2O$ matrix. The tables at the bottom of Figures (A) and (B) present the fractions of acetaldehyde in different phases obtained from the corresponding RAIR and TPD-MS spectra.

130−135 K and subsequent formation of ice $I_c$ were studied. The associated kinetics parameters and activation energy for the conversion of "the CH phase to ice $I_c$" were estimated.

Acetaldehyde CH was prepared by thermal annealing of an acetaldehyde−$H_2O$ (1:2) ice mixture under UHV. Figure 1A shows the temperature-dependent RAIR spectra of 300 ML of acetaldehyde−$H_2O$ (1:2) film in the C=O stretching region. The spectrum collected just after vapor deposition of the ice mixture at 10 K shows a peak at 1723 $cm^{-1}$, which is attributed to the interaction of acetaldehyde with water ice. When the ice mixture was annealed from 10 to 115 K, a peak at 1729 $cm^{-1}$ along with a shoulder at 1734 $cm^{-1}$ appeared (marked by vertical dashed lines). The peak at 1729 $cm^{-1}$ is due to the pure solid acetaldehyde, which was confirmed by comparing it with the RAIR spectrum of pure acetaldehyde, shown in Figure S1. This suggests that acetaldehyde got phase separated in the water matrix during annealing.[29] However, the shoulder at 1734 $cm^{-1}$ is an entirely new IR feature and is attributed to acetaldehyde CH. The basis of this assignment is some previous studies,[1,4,5,30,31] which suggest that the vibrational frequency of the guest molecules trapped in CH cages usually falls in between their condensed (1729 $cm^{-1}$) and vapor (1746 $cm^{-1}$)[32,33] phase frequencies. Therefore, the peak at 1734 $cm^{-1}$ in the C=O stretching region may be assigned to acetaldehyde CH. This assignment is further supported by the following observation. Upon further annealing the ice mixture to 135 K, the peak at 1723 $cm^{-1}$ vanished due to the desorption of phase-separated acetaldehyde from ice matrix, while the peak



https://doi.org/10.1021/acs.jpclett.3c01181
J. Phys. Chem. Lett. 2023, 14, 5328−5334

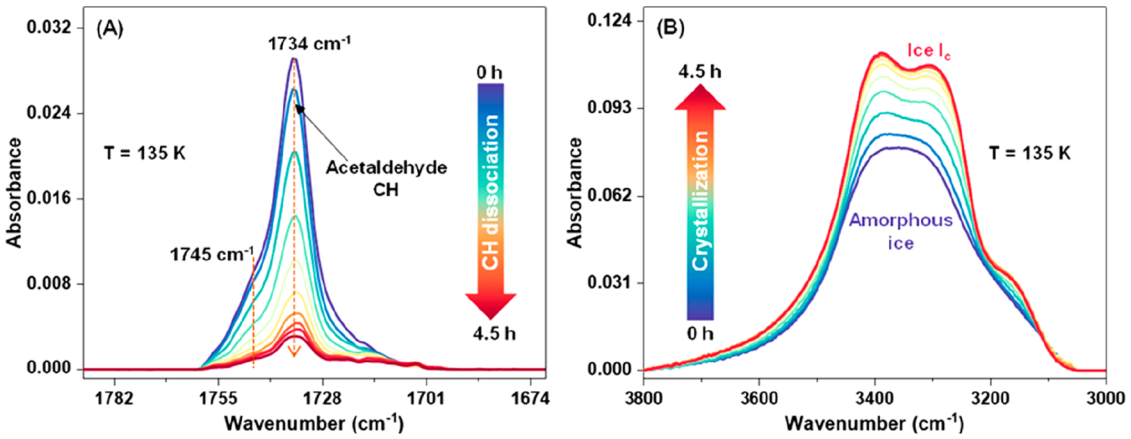


**Figure 3.** Ice $I_c$ formation via acetaldehyde CH. RAIR spectra of 300 ML of acetaldehyde–$H_2O$ (1:2) film at 135 K in the (A) C=O and (B) O–H stretching regions. The ice mixture was codeposited on a Ru(0001) substrate at 10 K and annealed at a rate of 2 K·min$^{-1}$ to 135 K. Upon isothermal annealing at 135 K, the peak at 1734 cm$^{-1}$ diminishes with time due to the dissociation of acetaldehyde CH, which resulted in ice $I_c$.

at 1734 cm$^{-1}$ remained because of the trapping of acetaldehyde in CH cages.[1,4,5] Notably, at higher temperatures, a small, broad peak at 1745 cm$^{-1}$ appeared (along with 1734 cm$^{-1}$), which was assigned to grain-boundary acetaldehyde,[34] in other words, acetaldehyde that was trapped into intergrain regions. The primary reason for this assignment is that the vibrational feature at 1745 cm$^{-1}$ is broad (due to a random distribution of acetaldehyde in the grain boundaries) and is very close to the gas phase vibrational feature (1746 cm$^{-1}$)[32,33] of acetaldehyde. Figure 1B illustrates schematically the stepwise physical change that occurs upon annealing the acetaldehyde–$H_2O$ (1:2) ice mixture from 10 to 135 K. Further, the stability of acetaldehyde CH was investigated in a separate time-dependent RAIRS experiment performed at 115 K for 27 h. The result presented in Figure S2A suggests that the acetaldehyde CH phase is not only stable at 115 K under UHV but also does not convert to the geminal diol.

To get a clearer picture and further confirm the CH formation, we have carried out a TPD experiment, and the outcome was correlated with the RAIRS results of the same sample. For this, we have prepared a 300 ML acetaldehyde–$H_2O$ (1:2) film at 10 K and annealed it to 137 K at a rate of 2 K·min$^{-1}$ to form acetaldehyde CH, free of phase-separated acetaldehyde (which would have desorbed during annealing as shown in Figure 1A). The prepared sample was cooled back to 10 K. Just after cooling back to 10 K, the RAIR spectrum was collected as shown in Figure 2A, which shows three peaks at 1745 cm$^{-1}$ (broad), 1734 cm$^{-1}$ (sharp), and ∼1723 cm$^{-1}$ (weak and broad) in the C=O stretching region, attributed to the grain-boundary acetaldehyde (32% of the total acetaldehyde present in ice matrix at this condition), acetaldehyde CH (55%), and a dilute mixture of acetaldehyde in water ice (13%), respectively. The table (below Figure 2A) shows the fractions of acetaldehyde in different phases, and they were obtained by deconvoluting the RAIR spectrum presented in Figure 2A. After IR spectral acquisition at 10 K, the sample was annealed at a rate of 30 K·min$^{-1}$ to 200 K, and the TPD spectrum was collected as shown in Figure 2B. The thermal desorption trace of acetaldehyde was obtained by plotting the intensity of $CHO^+$ ($m/z$ = 29) as a function of temperature. Figure 2B shows four desorption peaks at 128, 138, 146, and 161 K, which are attributed to the desorption of (1) acetaldehyde that is present in amorphous ice pores (12%), (2) acetaldehyde that was trapped in CH cages (54%), (3) grain-boundary acetaldehyde (31%), and (4) a small fraction of acetaldehyde that desorbs along with water (3%), respectively. Moreover, the TPD spectrum of pure acetaldehyde shows a desorption peak at ∼110 K, as shown in Figure S2B. In Figure 2B, the peak at 128 K is due to the premelting of ice that releases some (12%) of acetaldehyde present in the pores of ASW. The total fractions of acetaldehyde trapped in ASW matrix (12 + 3 = 15%) obtained from TPD experiment are comparable to that of 13% estimated from the RAIR spectrum shown in Figure 2A. The assignment of the peak at 146 K as due to grain-boundary acetaldehyde is because it coincides with the amorphous to crystalline transition of ice. When amorphous ice converts to crystalline ice above 140 K, due to the rearrangement of water molecules, the molecular species trapped in the amorphous pores/grain boundaries leave the ice matrix abruptly in an event known as a "molecular volcano", resulting in a sharp desorption peak of the corresponding species.[35,36] The peak at 146 K is sharp, which further supports our assignment. The remaining peak at 138 K was assigned to the desorption of acetaldehyde that is trapped in CH cages. This assignment was confirmed by comparing the estimated fractions of acetaldehyde trapped in CH cages obtained from the RAIRS and TPD measurements (see the Tables listed in Figure 2). A good agreement of the fractions of acetaldehyde of different phases estimated from the RAIRS and TPD measurements of the same sample further justified our assignments. Thus, for the first time, we report the formation of stable CH of acetaldehyde prepared under UHV and cryogenic conditions.

CHs are known to dissociate to different crystalline structures.[4,5,7,8] To explore this possibility, we have carried out a time-dependent RAIRS experiment with 300 ML of acetaldehyde–$H_2O$ (1:2) film at 135 K. The results obtained in the (A) C=O and (B) O–H stretching regions are shown in Figure 3A,B, respectively. Figure 3A shows that after keeping the ice sample at 135 K for 4.5 h, the acetaldehyde CH peak at 1734 cm$^{-1}$ (along with 1745 cm$^{-1}$) in the C=O stretching region decreases due to CH dissociation. In a similar time scale, the O–H stretching band shown in Figure 3B shows a profound change due to the dissociation of acetaldehyde CH. At 0 h, the broad feature in the O–H stretching region, which is characteristic of amorphous ice, undergoes splitting within 4.5 h. The splitting of the O–H stretching band in the IR spectra is associated with the crystallization of the water ice


https://doi.org/10.1021/acs.jpclett.3c01181
J. Phys. Chem. Lett. 2023, 14, 5328–5334

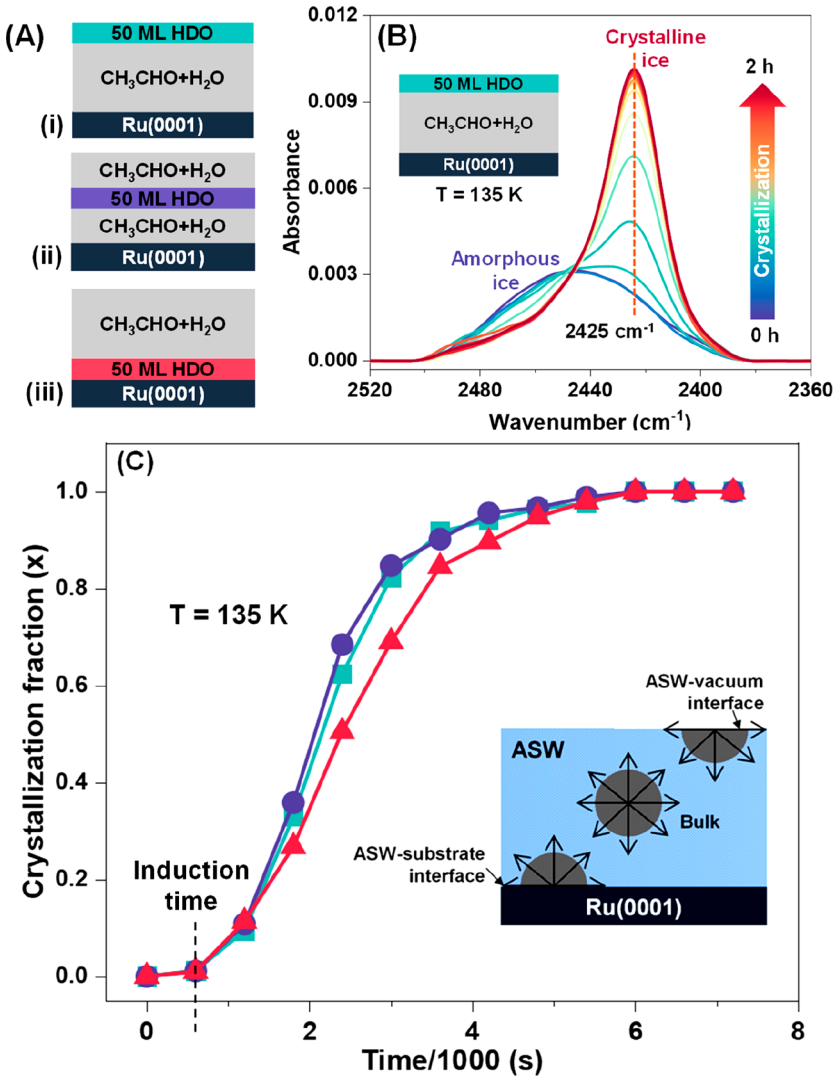


**Figure 4.** Isothermal RAIRS measurement of the crystallization fraction of a 50 ML HDO layer embedded in 200 ML acetaldehyde–$H_2O$ (1:10) film at 135 K. (A) Structure of composite ice film containing a 50 ML HDO layer at specific positions in a 200 ML acetaldehyde–$H_2O$ (1:10) film, namely, at the top (green layer), in the bulk (blue layer), and at the bottom (red layer). Acetaldehyde–$H_2O$ (1:10) film is indicated by gray layers. (B) Changes in the O–D stretching band of 50 ML HDO, at 135 K with time, shown for the composite film with the HDO layer at the top. (C) Crystallization fraction versus time curves for the 50 ML HDO layer embedded at various positions in the 200 ML acetaldehyde–$H_2O$ (1:10) film. The CF was calculated from a vertical cut at 2425 $cm^{-1}$ in the O–D stretching band of the isothermal RAIR spectra shown in B and Figure S5. The inset of C shows the possibilities of the onset of ASW crystallization, which may initiate at interfaces or in the bulk.

film.[4,37−39] The spectrum after 4.5 h is attributed to the formation of ice $I_c$. This assignment was confirmed by comparing the spectrum with the IR spectrum of our previous work[4] (shown in Figure S3) where cubic ice was prepared using acetone CH. It was confirmed by reflection high energy electron diffraction (RHEED). The RAIR spectra in the O–H stretching region (Figure S3) confirmed the formation of ice $I_c$ after the dissociation of acetaldehyde CH at 135 K. However, 150 ML of pure ASW does not undergo crystallization at 130–135 K in similar experimental conditions. Results of isothermal annealing of ASW are shown in Figure S4. We conclude that acetaldehyde CH at 135 K under UHV dissociates to form cubic crystalline ice.

To understand the mechanism of CH dissociation and subsequent crystalline ice formation during isothermal experiments, we have carried out an experiment using the "selective placement method".[39,40] For this, in three different experiments (see the Experimental Section for details of sample preparation), we placed a 50 ML HDO (5% $D_2O$ in $H_2O$) probe layer in 200 ML acetaldehyde–$H_2O$ (1:10) films at specific positions as shown in Figure 4A and evaluated the crystallization fraction by monitoring the evolution in the O–D stretching band of the HDO layer (shown in Figures 4B and S5) at 135 K as a function of crystallization time. Figure 4C shows the change in the crystallization fraction of the 50 ML HDO layer placed at different positions in the 200 ML acetaldehyde–$H_2O$ (1:10) film at the top (green curve), middle (blue curve), and bottom (red curve). Crystallization fractions were calculated from a vertical cut at 2425 $cm^{-1}$ in the O–D stretching band shown in Figures 4B and S5; the first spectrum in each case is from completely amorphous film and the final spectrum is from the completely crystalline film, while the intermediate spectra are a linear combination of amorphous and crystalline spectra. Figure 4C shows that the HDO probe layer placed in the bulk (blue curve) and at the ice–vacuum interface (green curve) crystallized almost at the



https://doi.org/10.1021/acs.jpclett.3c01181
J. Phys. Chem. Lett. 2023, 14, 5328−5334

Table 1. Kinetics Parameters Estimated Using the Avrami Equation at Various Temperatures

| Temperature | 130 K | 132 K | 135 K | 137 K |
|---|---|---|---|---|
| ln ($k$) | 9.2 ± 0.7 | 8.5 ± 0.7 | 7.9 ± 0.9 | 6.3 ± 1.9 |
| $n$ | 2.64 ± 0.10 | 2.13 ± 0.09 | 1.96 ± 0.12 | 1.89 ± 0.27 |

same speed. This suggests that the crystallization initiates at random nucleation sites in bulk and propagates in all directions; that is why the HDO probe layer placed at the bulk and ice−vacuum interface crystallizes at the same speed. This, in turn, implies that the acetaldehyde CHs are distributed all over the ice matrix, and during isothermal annealing, CH dissociates at random places (independent of site, namely in bulk or at interfaces) and induces ASW crystallization. However, the HDO layer placed at the bottom (red curve) of the acetaldehyde−$H_2O$ (1:10) film crystallizes last and with slower kinetics. The reason for this is that the fraction of acetaldehyde CH present in the HDO layer placed at the bottom will be less compared to the other two cases. This is because, during thermal annealing, the possibility of acetaldehyde diffusion and subsequent CH formation in the HDO layer is least among the cases shown in Figure 4A. In conclusion, under UHV and cryogenic conditions, acetaldehyde CH was found to be distributed throughout the ASW matrix in the form of small domains (instead of an extended crystalline phase), and its dissociation leads to the crystallization of ASW which initiates in the bulk, at random locations.

Notably, in Figure 4C, each curve has an induction time of ∼10 min. In other words, ASW crystallization starts after 10 min of isothermal annealing of the sample at 135 K. However, acetaldehyde CH dissociation (reduction in the intensity of 1734 $cm^{-1}$) at 135 K starts from 0 min as shown in Figure S6. That means, at first, CH dissociation takes place followed by the onset of ASW crystallization. It confirms our interpretation of the 138 and 146 K peaks in TPD-MS data (shown in Figure 2B) as due to the desorption of acetaldehyde trapped in CH cages and grain boundaries, respectively. This is explained by the fact that at ∼138 K CH dissociates leading to the desorption of acetaldehyde, and this initiates the crystallization of ASW. During ASW crystallization, water molecules undergo rearrangement, which will lead to the desorption of acetaldehyde that exists in grain boundaries of the ASW matrix at temperatures >140 K.

Our claim of acetaldehyde CH formation and subsequent crystallization of ASW to ice $I_c$ was further confirmed in several control experiments. (1) A temperature-dependent RAIRS experiment with acetaldehyde−$D_2O$ (1:2) film was caried out, and the results are shown in Figure S7. Figure S7 shows that acetaldehyde forms CH with $D_2O$, and its subsequent dissociation leads to the formation of ice $I_c$. (2) A temperature-dependent RAIRS experiment with sequentially deposited acetaldehyde@$H_2O$ film also resulted in acetaldehyde CH followed by ice $I_c$ at higher temperatures (Figure S8). Further, considering the cometary environment where such guest molecules are less abundant, we have performed a time-dependent RAIRS experiment with dilute mixtures of acetaldehyde−$H_2O$ (1:20 and 1:40) at 135 K. The results from these two experiments (Figures S9 and S10) show the formation of acetaldehyde CH and subsequent ice $I_c$.

Kinetic parameters of ice $I_c$ crystallization via acetaldehyde CH were evaluated using the Avrami equation by conducting time-dependent RAIRS experiments with 300 ML of acetaldehyde−$H_2O$ (1:10) film in the temperature range of 130−135 K (Figure S11).[41,42] The methods utilized for the estimation of various kinetic parameters for ice $I_c$ crystallization are the same as discussed in our previous papers[4,5,38,39] and are briefly described in the Supporting Information. Table 1 summarizes the estimated crystallization rate constant ($k$) and Avrami exponent ($n$) at various temperatures evaluated from the time-dependent RAIR spectra shown in Figure S11. At higher temperatures, because of fast CH dissociation, the rate of crystallization will be faster. The estimated values of $n$ (2.64−1.89) shown in Table 1 are consistent with the $n$ values of our previous study of ice $I_c$ formation via CH dissociation.[4] The values of $n$ suggest that the crystallization kinetics is diffusion-controlled with particles growing into a predominantly spherical geometry.[4,43−45] Further, the activation energy ($E_a$) of crystallization was estimated (see the details in Supporting Information). The estimated value was 56.6 kJ $mol^{-1}$ and is comparable to the previously reported[40,46−49] activation energy values (60−77 kJ $mol^{-1}$) for the crystallization of pure ASW. This implies that even at low temperatures, the CH dissociation causes enough mobility for the water molecules to overcome the kinetic barrier of crystallization.

In conclusion, we report the existence of elusive acetaldehyde CH under UHV and cryogenic temperatures. We found that acetaldehyde in its ice mixture with water forms CH at 115 K, and the CH phase remains beyond 27 h without converting to a geminal diol. The conversion of acetaldehyde CH to ice $I_c$ (at 130−135 K) and the associated mechanism and kinetics were also studied. Ice $I_c$ via acetaldehyde CH could be one of the routes for the formation of this phase in comets, as ice $I_c$ and CH are reported to exist in such environments.[27,28,50] While our study established the possibility of several similar molecules in the CH phase, it also points to the existence of such molecular solids in comets, planets, and interstellar environment. The consequence of the CH in deciding the molecular composition of such environments needs further investigation.

## ■ ASSOCIATED CONTENT

### Supporting Information

The Supporting Information is available free of charge at https://pubs.acs.org/doi/10.1021/acs.jpclett.3c01181.

Experimental Section (including apparatus, materials and reagents, sample preparation, experimental procedure, RAIRS and TPD-MS setup), temperature- and time-dependent RAIR spectra of pure acetaldehyde and acetaldehyde−$H_2O$ films, time-dependent RAIR spectra of acetaldehyde−$H_2O$ films (in different ratios) at different temperatures, TPD-MS spectra of pure acetaldehyde, crystallization kinetics (PDF)

## ■ AUTHOR INFORMATION

### Corresponding Author

**Thalappil Pradeep** − *DST Unit of Nanoscience (DST UNS) and Thematic Unit of Excellence (TUE), Department of*



https://doi.org/10.1021/acs.jpclett.3c01181
J. Phys. Chem. Lett. 2023, 14, 5328−5334

*Chemistry, Indian Institute of Technology Madras, Chennai 600036, India; International Centre for Clean Water, IIT Madras Research Park, Chennai 600113, India;* orcid.org/0000-0003-3174-534X; Email: pradeep@iitm.ac.in

### Authors

**Gaurav Vishwakarma** − *DST Unit of Nanoscience (DST UNS) and Thematic Unit of Excellence (TUE), Department of Chemistry, Indian Institute of Technology Madras, Chennai 600036, India*

**Bijesh K. Malla** − *DST Unit of Nanoscience (DST UNS) and Thematic Unit of Excellence (TUE), Department of Chemistry, Indian Institute of Technology Madras, Chennai 600036, India*

**Soham Chowdhury** − *DST Unit of Nanoscience (DST UNS) and Thematic Unit of Excellence (TUE), Department of Chemistry, Indian Institute of Technology Madras, Chennai 600036, India*

**Sakshi Pradip Khandare** − *DST Unit of Nanoscience (DST UNS) and Thematic Unit of Excellence (TUE), Department of Chemistry, Indian Institute of Technology Madras, Chennai 600036, India*

Complete contact information is available at: https://pubs.acs.org/10.1021/acs.jpclett.3c01181

### Author Contributions

T.P. and G.V. designed the research. T.P. supervised its progress. G.V., B.K.M., S.C., and S.P.K. have performed the experiments. G.V., B.K.M., S.C., S.P.K., and T.P. have analyzed the results. The first draft of manuscript is written by G.V. The final version of manuscript was written with the contributions of all authors.

### Notes

The authors declare no competing financial interest.

## ■ ACKNOWLEDGMENTS

We acknowledge the Science and Engineering Research Board (SERB), Department of Science and Technology (DST), Government of India for research funding. T.P. acknowledges funding from the Centre of Excellence on Molecular Materials and Functions under the Institution of Eminence scheme of IIT Madras. G.V. and S.C. thank IITM for their research fellowships. B.K.M. thanks the Council of Scientific & Industrial Research (CSIR) for his research fellowship.

## ■ REFERENCES

(1) Ghosh, J.; Methikkalam, R. R. J.; Bhuin, R. G.; Ragupathy, G.; Choudhary, N.; Kumar, R.; Pradeep, T. Clathrate Hydrates in Interstellar Environment. *Proc. Natl. Acad. Sci. U. S. A.* **2019**, *116*, 1526−1531.

(2) Vishwakarma, G.; Malla, B. K.; Reddy, K. S. S. V. P.; Ghosh, J.; Chowdhury, S.; Yamijala, S. S. R. K. C.; Reddy, S. K.; Kumar, R.; Pradeep, T. Induced Migration of CO2 from Hydrate Cages to Amorphous Solid Water under Ultrahigh Vacuum and Cryogenic Conditions. *J. Phys. Chem. Lett.* **2023**, *14*, 2823−2829.

(3) Malla, B. K.; Vishwakarma, G.; Chowdhury, S.; Selvarajan, P.; Pradeep, T. Formation of Ethane Clathrate Hydrate in Ultrahigh Vacuum by Thermal Annealing. *J. Phys. Chem. C* **2022**, *126*, 17983−17989.

(4) Ghosh, J.; Bhuin, R. G.; Vishwakarma, G.; Pradeep, T. Formation of Cubic Ice via Clathrate Hydrate, Prepared in Ultrahigh Vacuum under Cryogenic Conditions. *J. Phys. Chem. Lett.* **2020**, *11*, 26−32.

(5) Ghosh, J.; Vishwakarma, G.; Das, S.; Pradeep, T. Facile Crystallization of Ice $I_h$ via Formaldehyde Hydrate in Ultrahigh Vacuum under Cryogenic Conditions. *J. Phys. Chem. C* **2021**, *125*, 4532−4539.

(6) Ghosh, J.; Bhuin, R. G.; Ragupathy, G.; Pradeep, T. Spontaneous Formation of Tetrahydrofuran Hydrate in Ultrahigh Vacuum. *J. Phys. Chem. C* **2019**, *123*, 16300−16307.

(7) Kuhs, W. F.; Genov, G.; Staykova, D. K.; Hansen, T. Ice Perfection and Onset of Anomalous Preservation of Gas Hydrates. *Phys. Chem. Chem. Phys.* **2004**, *6*, 4917−4920.

(8) Falenty, A.; Kuhs, W. F. Self-Preservation" of CO2 Gas Hydrates-Surface Microstructure and Ice Perfection. *J. Phys. Chem. B* **2009**, *113*, 15975−15988.

(9) Komatsu, K.; Machida, S.; Noritake, F.; Hattori, T.; Sano-Furukawa, A.; Yamane, R.; Yamashita, K.; Kagi, H. Ice Ic without Stacking Disorder by Evacuating Hydrogen from Hydrogen Hydrate. *Nat. Commun.* **2020**, *11*, 464.

(10) Falenty, A.; Hansen, T. C.; Kuhs, W. F. Cubic Ice Formation and Annealing during CO2 Clathrate Hydrate Decomposition at Low Temperatures; Hokkaido Univ Press: Sapporo, 2010.

(11) Takeya, S.; Uchida, T.; Nagao, J.; Ohmura, R.; Shimada, W.; Kamata, Y.; Ebinuma, T.; Narita, H. Particle Size Effect of CH4 Hydrate for Self-Preservation. *Chem. Eng. Sci.* **2005**, *60*, 1383−1387.

(12) Falenty, A.; Hansen, T. C.; Kuhs, W. F. Formation and Properties of Ice XVI Obtained by Emptying a Type SII Clathrate Hydrate. *Nature* **2014**, *516*, 231−233.

(13) Bauer, R. P. C.; Ravichandran, A.; Tse, J. S.; Appathurai, N.; King, G.; Moreno, B.; Desgreniers, S.; Sammynaiken, R. In Situ X-Ray Diffraction Study on Hydrate Formation at Low Temperature in a High Vacuum. *J. Phys. Chem. C* **2021**, *125*, 26892−26900.

(14) Sloan, E. D. Fundamental Principles and Applications of Natural Gas Hydrates. *Nature* **2003**, *426*, 353−359.

(15) Davidson, D. W.; Gough, S. R.; Ripmeester, J. A. Dielectric and Nuclear Magnetic Resonance Characterization of Unstable Clathrate Hydrates of Acetaldehyde and Propionaldehyde. *Can. J. Chem.* **1976**, *54*, 3085−3088.

(16) Kang, H.; Ahn, Y. H.; Koh, D. Y.; Lee, H. Thermodynamic and Spectroscopic Identification of Aldehyde Hydrates. *Korean J. Chem. Eng.* **2016**, *33*, 1897−1902.

(17) Bell, R. P.; Clunie, J. C. The Hydration of Acetaldehyde in Aqueous Solution. *Trans. Faraday Soc.* **1952**, *48*, 439−442.

(18) Matsushima, M. The Hydration of Some Organic Compounds in an Aqueous Solution. I. Studies of Aliphatic Aldehydes by Raman-Effect Observation. *Bull. Chem. Soc. Jpn.* **1963**, *36*, 954−960.

(19) Kurz, J. L. The Hydration of Acetaldehyde. I. Equilibrium Thermodynamic Parameters. *J. Am. Chem. Soc.* **1967**, *89*, 3524−3528.

(20) Petrenko, V.; Whitworth, R. *Physics of Ice*; Oxford University Press, 2002.

(21) Jenniskens, P.; Blake, D. F. Crystallization of Amorphous Water Ice in the Solar System. *Astrophys. J.* **1996**, *473*, 1104−1113.

(22) Lobban, C.; Finney, J. L.; Kuhs, W. F. The Structure of a New Phase of Ice. *Nature* **1998**, *391*, 268−270.

(23) del Rosso, L.; Celli, M.; Grazzi, F.; Catti, M.; Hansen, T. C.; Fortes, A. D.; Ulivi, L. Cubic Ice Ic without Stacking Defects Obtained from Ice XVII. *Nat. Mater.* **2020**, *19*, 663−668.

(24) Davies, M. B.; Fitzner, M.; Michaelides, A. Routes to Cubic Ice through Heterogeneous Nucleation. *Proc. Natl. Acad. Sci. U. S. A.* **2021**, *118*, e2025245118.

(25) Huang, X.; Wang, L.; Liu, K.; Liao, L.; Sun, H.; Wang, J.; Tian, X.; Xu, Z.; Wang, W.; Liu, L.; Jiang, Y.; Chen, J.; Wang, E.; Bai, X. Tracking Cubic Ice at Molecular Resolution. *Nature* **2023**, *617*, 86−91.

(26) Kuhs, W. F.; Sippel, C.; Falenty, A.; Hansen, T. C. Extent and Relevance of Stacking Disorder in "Ice Ic. *Proc. Natl. Acad. Sci. U. S. A.* **2012**, *109*, 21259−21264.

(27) Luspay-Kuti, A.; Mousis, O.; Hässig, M.; Fuselier, S. A.; Lunine, J. I.; Marty, B.; Mandt, K. E.; Wurz, P.; Rubin, M. The Presence of Clathrates in Comet 67P/Churyumov-Gerasimenko. *Sci. Adv.* **2016**, *2*, No. e1501781.

(28) Prialnik, D.; Bar-Nun, A. Crystallization of Amorphous Ice as the Cause of Comet P/Halley's Outburst at 14 AU. *Astron. Astrophys.* **1992**, *258*, L9−L12.
(29) Bhuin, R. G.; Methikkalam, R. R. J.; Sivaraman, B.; Pradeep, T. Interaction of Acetonitrile with Water-Ice: An Infrared Spectroscopic Study. *J. Phys. Chem. C* **2015**, *119*, 11524−11532.
(30) Buch, V.; Devlin, J. P.; Monreal, I. A.; Jagoda-Cwiklik, B.; Uras-Aytemiz, N.; Cwiklik, L. Clathrate Hydrates with Hydrogen-Bonding Guests. *Phys. Chem. Chem. Phys.* **2009**, *11*, 10245−10265.
(31) Subramanian, S.; Sloan, E. D. Trends in Vibrational Frequencies of Guests Trapped in Clathrate Hydrate Cages. *J. Phys. Chem. B* **2002**, *106*, 4348−4355.
(32) Ito, F. Matrix-Isolation Infrared Study of Acetaldehyde: Host-Dependent Vibrational Features. *J. Mol. Spectrosc.* **2022**, *384*, 111593.
(33) Ding, Y.; Peng, W. Y.; Strand, C. L.; Hanson, R. K. Quantitative Measurements of Broad-Band Mid-Infrared Absorption Spectra of Formaldehyde, Acetaldehyde, and Acetone at Combustion-Relevant Temperatures near 5.7 Mm. *J. Quant. Spectrosc. Radiat. Transfer* **2020**, *248*, 106981.
(34) Kondo, T.; Kato, H. S.; Kawai, M.; Bonn, M. The Distinct Vibrational Signature of Grain-Boundary Water in Nano-Crystalline Ice Films. *Chem. Phys. Lett.* **2007**, *448*, 121−126.
(35) May, R. A.; Smith, R. S.; Kay, B. D. The Release of Trapped Gases from Amorphous Solid Water Films. I. "Top-down" Crystallization-Induced Crack Propagation Probed Using the Molecular Volcano. *J. Chem. Phys.* **2013**, *138*, 104501.
(36) May, R. A.; Smith, R. S.; Kay, B. D. Probing the Interaction of Amorphous Solid Water on a Hydrophobic Surface: Dewetting and Crystallization Kinetics of ASW on Carbon Tetrachloride. *Phys. Chem. Chem. Phys.* **2011**, *13*, 19848−19855.
(37) Backus, E. H. G.; Grecea, M. L.; Kleyn, A. W.; Bonn, M. Surface Crystallization of Amorphous Solid Water. *Phys. Rev. Lett.* **2004**, *92*, 236101.
(38) Vishwakarma, G.; Ghosh, J.; Pradeep, T. Desorption-Induced Evolution of Cubic and Hexagonal Ices in an Ultrahigh Vacuum and Cryogenic Temperatures. *Phys. Chem. Chem. Phys.* **2021**, *23*, 24052−24060.
(39) Vishwakarma, G.; Malla, B. K.; Methikkalam, R. R. J.; Pradeep, T. Rapid Crystallization of Amorphous Solid Water by Porosity Induction. *Phys. Chem. Chem. Phys.* **2022**, *24*, 26200−26210.
(40) Lee, D. H.; Kang, H. Acid-Promoted Crystallization of Amorphous Solid Water. *J. Phys. Chem. C* **2018**, *122*, 24164−24170.
(41) Avrami, M. Kinetics of Phase Change. I: General Theory. *J. Chem. Phys.* **1939**, *7*, 1103−1112.
(42) Avrami, M. Kinetics of Phase Change. II Transformation-Time Relations for Random Distribution of Nuclei. *J. Chem. Phys.* **1940**, *8*, 212−224.
(43) Hage, W.; Hallbrucker, A.; Mayer, E.; Johari, G. P. Crystallization Kinetics of Water below 150 K. *J. Chem. Phys.* **1994**, *100*, 2743−2747.
(44) Rao, C. N. R.; Rao, K. J. *Phase Transitions in Solids: An Approach to the Study of the Chemistry and Physics of Solids*; McGraw-Hill: New York, 1978.
(45) Doremus, R. H. *Rates of Phase Transformations*; Academic Press: New York, 1985.
(46) Kondo, T.; Kato, H. S.; Bonn, M.; Kawai, M. Deposition and Crystallization Studies of Thin Amorphous Solid Water Films on Ru(0001) and on CO-Precovered Ru(0001). *J. Chem. Phys.* **2007**, *127*, 094703.
(47) Safarik, D. J.; Mullins, C. B. The Nucleation Rate of Crystalline Ice in Amorphous Solid Water. *J. Chem. Phys.* **2004**, *121*, 6003−6010.
(48) Smith, R. S.; Matthiesen, J.; Knox, J.; Kay, B. D. Crystallization Kinetics and Excess Free Energy of H2O and D2O Nanoscale Films of Amorphous Solid Water. *J. Phys. Chem. A* **2011**, *115*, 5908−5917.
(49) Yuan, C.; Smith, R. S.; Kay, B. D. Communication: Distinguishing between Bulk and Interface-Enhanced Crystallization in Nanoscale Films of Amorphous Solid Water. *J. Chem. Phys.* **2017**, *146*, 031102.
(50) Gronkowski, P. The Search for a Cometary Outbursts Mechanism: A Comparison of Various Theories. *Astron. Nachrichten* **2007**, *328*, 126−136.


https://doi.org/10.1021/acs.jpclett.3c01181
*J. Phys. Chem. Lett.* 2023, 14, 5328−5334